4698 *Inorg. Chem.* **2010**, *49*, 4698–4707
DOI: 10.1021/ic1003534

Inorganic Chemistry
Article

Germanium(II) and Tin(II) Complexes of a Sterically Demanding Phosphanide Ligand

Keith Izod,* John Stewart, Ewan R. Clark, William Clegg, and Ross W. Harrington

Main Group Chemistry Laboratories, School of Chemistry, Bedson Building, University of Newcastle, Newcastle upon Tyne, NE1 7RU, U.K.

Received February 22, 2010

The reaction between $PhPCl_2$ and 1 equiv of RLi, followed by in situ reduction with $LiAlH_4$ and an aqueous workup yields the secondary phosphane PhRPH [R = $(Me_3Si)_2CH$]. Treatment of PhRPH with *n*-BuLi in diethyl ether generates the lithium phosphanide $(RPhP)Li(Et_2O)_n$ [**15**(Et_2O)], which may be crystallized as the tetrahydrofuran (THF) adduct $(RPhP)Li(THF)_3$ [**15**(THF)]. Compound **15**(Et_2O) reacts with 1 equiv of either NaO-*t*Bu or KO-*t*Bu to give the corresponding sodium and potassium phosphanides $(RPhP)Na(Et_2O)_n$ (**16**) and $(RPhP)K(Et_2O)_n$ (**17**), which may be crystallized as the amine adducts $[(RPhP)Na(tmeda)]_2$ [**16**(tmeda)] and $[(RPhP)K(pmdeta)]_2$ [**17**(pmdeta)], respectively. The reaction between 2 equiv of **17** and $GeCl_2$(1,4-dioxane) gives the dimeric compound $[(RPhP)_2Ge]_2 \cdot Et_2O$ (**18** $\cdot Et_2O$). In contrast, the reaction between 2 equiv of **15** and $SnCl_2$ preferentially gives the ate complex $(RPhP)_3SnLi(THF)$ (**19**) in low yield; **19** is obtained in quantitative yield from the reaction between $SnCl_2$ and 3 equiv of **15**. Crystallization of **19** from *n*-hexane/THF yields the separated ion pair complex $[(RPhP)_3Sn][Li(THF)_4]$ (**19a**); exposure of **19a** to vacuum for short periods leads to complete conversion to **19**. Treatment of $GeCl_2$(1,4-dioxane) with 3 equiv of **15** yields the contact ion pair $(RPhP)_3GeLi(THF)$ (**20**), after crystallization from *n*-hexane/THF. Compounds **15**(THF), **16**(tmeda), **17**(pmdeta), **18** $\cdot Et_2O$, **19a**, and **20** have been characterized by elemental analyses, multielement NMR spectroscopy, and X-ray crystallography. While **15**(THF) is monomeric, both **16**(tmeda) and **17**(pmdeta) are dimeric in the solid state. The diphosphagermylene **18** $\cdot Et_2O$ adopts a dimeric structure in the solid state with a *syn*,*syn*-arrangement of the phosphanide ligands, and this structure appears to be preserved in solution. The ate complex **19a** crystallizes as a separated ion pair, whereas the analogous ate complex **20** crystallizes as a discrete molecular species. The structures of **19** and **20** are retained in non-donor solvents, while dissolution in THF yields the separated ion pairs **19a** and $[(RPhP)_3Ge][Li(THF)_4]$ (**20a**).

Introduction

Whereas the heavier group 14 analogues of diaminocarbenes [diaminotetrylenes; $(R_2N)_2E$, E = Si, Ge, Sn, Pb] have been known for many years and are well established, the corresponding diphosphatetrylenes [$(R_2P)_2E$] have been less well explored.[1,2] Structurally characterized monomeric diphosphatetrylenes are limited to the highly sterically hindered compounds $[\{(Tripp)_2FSi\}(iPr_3Si)P]_2E$ [E = Ge (**1**), Sn (**2**), Pb; Tripp = 2,4,6-$iPr_3C_6H_2$][3] reported by Driess and co-workers, although Power and co-workers have reported the spectroscopically characterized monomeric diphosphastannylene $[\{2,6\text{-}(2,4,6\text{-}Me_3C_6H_2)_2C_6H_3\}(Ph)P]_2Sn$ (**3**) (Chart 1).[4] The remaining crystallographically characterized diphosphatetrylenes, $\{(tBu_2P)_2Pb\}_2$ (**4**),[5] $\{((Me_3Si)_2P)_2Pb\}_2$ (**5**),[6] and $\{(iPr_2P)_2Ge\}_2$ (**6**),[7] are dimeric both in the solid state and in solution. In addition, the ate complexes $(tBu_2P)E(\mu\text{-}tBu_2P)_2Li(THF)$ [E = Sn (**7**), Pb (**8**)] have been reported,[8] along with the heteroleptic species $\{(\mu_2\text{-}tBu_2P)GeCl\}_2$ (**9**)[7] and the β-diketiminate-supported phosphagermylenes $[CH\{(CMe)(2,6\text{-}iPr_2C_6H_3N)\}_2]Ge(PR_2)$ [PR_2 = PH_2, $PH(SiMe_3)$, $P(SiMe_3)_2$, 1/2(PH-PH)];[9] a range of homometallic Sn(II) phosphinidene clusters and heterometallic Ca/Sn or Ba/Sn phosphanide and phosphinidene clusters are also known.[10]

We have recently begun to explore the use of sterically demanding, donor-functionalized phosphanides such as $[\{(Me_3Si)_2CH\}(C_6H_4\text{-}2\text{-}(CH_2)_nNMe_2)P]^-$ (n = 0, 1) as ligands for low oxidation state group 14 centers. In our initial experiments we have shown that the compounds $[\{(Me_3Si)_2CH\}(C_6H_4\text{-}2\text{-}CH_2NMe_2)P]_2E$ [E = Ge (**10**),[11] Sn (**11**)[12]] and

*To whom correspondence should be addressed. E-mail: k.j.izod@ncl.ac.uk.

(1) For recent reviews of heavier tetrylene chemistry see: (a) Barrau, J.; Rima, G. *Coord. Chem. Rev.* **1998**, *178*−*180*, 593. (b) Tokitoh, N.; Okazaki, R. *Coord. Chem. Rev.* **2000**, *210*, 251. (c) Kira, M. *J. Organomet. Chem.* **2004**, *689*, 4475. (d) Weidenbruch, M. *Eur. J. Inorg. Chem.* **1999**, 373. (e) Klinkhammer, K. W. In *Chemistry of Organic Germanium, Tin and Lead Compounds*; Rappoport, Z., Ed; Wiley: New York, 2002; Vol. *2*, pp 283−357. (f) Veith, M. *Angew. Chem., Int. Ed. Engl.* **1987**, *26*, 1. (g) Hill, N. J.; West, R. *J. Organomet. Chem.* **2004**, *689*, 4165. (h) Gehrhus, B.; Lappert, M. F. *J. Organomet. Chem.* **2001**, *617*, 209. (i) Kühl, O. *Coord. Chem. Rev.* **2004**, *248*, 411. (j) Zemlyanskii, N. N.; Borisova, I. V.; Nechaev, M. S.; Khrustalev, V. N.; Lunin, V. V.; Antipin, M. Yu.; Ustynyuk, Yu. A. *Russ. Chem. Bull. Int. Ed.* **2004**, *53*, 980. (k) Zabula, A. V.; Hahn, F. E. *Eur. J. Inorg. Chem.* **2008**, 5165.

 Published on Web 04/14/2010

Chart 1

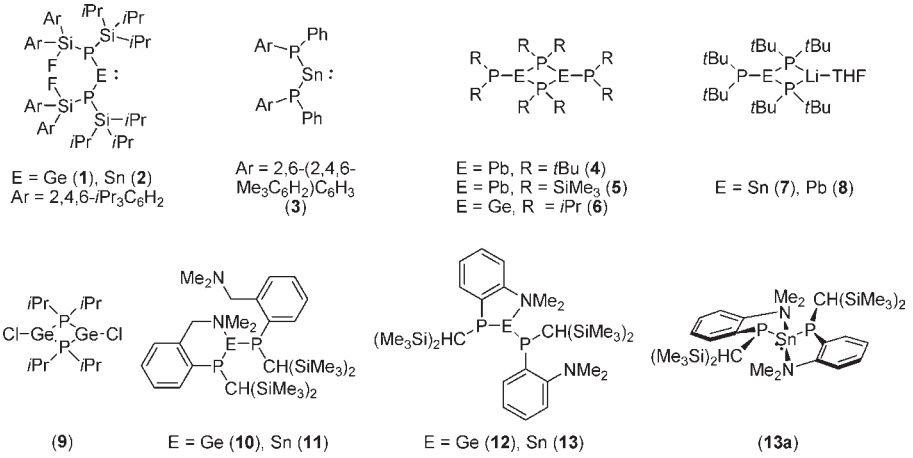

$[\{(Me_3Si)_2CH\}(C_6H_4\text{-}2\text{-}NMe_2)P]_2E$ [E = Ge (**12**), Sn (**13**)][13] are monomeric both in the solid state and in solution by virtue of the intramolecular coordination of one of the peripheral amino substituents in each case. Compounds **10**−**13** are highly dynamic in solution; detailed NMR studies and density functional theory (DFT) calculations suggest that these compounds are subject to both epimerization via inversion at one or more of the phosphorus centers and interconversion between the chelating and terminal phosphanide ligands. Low temperature NMR spectra indicate that compound **13** adopts a pseudotrigonal bipyramidal structure (**13a**) in solution which corresponds to the intermediate proposed for exchange of the chelating and terminal phosphanide ligands via an associative pathway.

We now report the synthesis of a related sterically hindered phosphane, $\{(Me_3Si)_2CH\}(Ph)PH$ (**14**), which does not contain additional donor functionality, the preparation and crystal structures of its lithium, sodium and potassium derivatives, and the reactions between these derivatives and either $GeCl_2$(1,4-dioxane) or $SnCl_2$ to give either diphosphatetrylenes or ate complexes.

Results and Discussion

The reaction between $PhPCl_2$ and 1 equiv of $[(Me_3Si)_2CH]Li$ in diethyl ether yields the monochlorophosphane $\{(Me_3Si)_2CH\}(Ph)PCl$, which, on treatment with $LiAlH_4$, gives the secondary phosphane $\{(Me_3Si)_2CH\}(Ph)PH$ (**14**) in good yield as a colorless oil. Treatment of **14** with *n*-BuLi in diethyl ether gives the lithium phosphanide $[\{(Me_3Si)_2CH\}(Ph)P]Li(Et_2O)_n$ [**15**(Et_2O)] as an orange oil which may be crystallized from cold *n*-hexane/tetrahydrofuran (THF) as the adduct $[\{(Me_3Si)_2CH\}(Ph)P]Li(THF)_3$ [**15**(THF)] (Scheme 1). The reaction between in situ prepared **15**(Et_2O) and either NaO-*t*Bu or KO-*t*Bu in diethyl ether gives the corresponding heavier alkali metal phosphanides $[\{(Me_3Si)_2CH\}(Ph)P]M$ [M = Na (**16**); M = K (**17**)], which may be crystallized as the adducts $[[\{(Me_3Si)_2CH\}(Ph)P]Na(tmeda)]_2$ [**16**(tmeda)] and $[[\{(Me_3Si)_2CH\}(Ph)P]K(pmdeta)]_2$ [**17**(pmdeta)] from methylcyclohexane containing 1 equiv of either tmeda or pmdeta, respectively [tmeda = *N*,*N*,*N*′,*N*′-tetramethylethylenediamine, pmdeta = *N*,*N*,*N*′,*N*″,*N*″-pentamethyldiethylenetriamine]. The ^1H, $^{13}C\{^1H\}$, and $^{31}P\{^1H\}$ NMR spectra of **14**, **15**(THF), **16**(tmeda), and **17**(pmdeta) are as expected. Whereas the $SiMe_3$ groups of **14** are diastereotopic, giving

(2) For selected references to diamidotetrylenes see: (a) Driess, M.; Yao, S.; Brym, M.; van Wullen, C.; Lentz, D. *J. Am. Chem. Soc.* **2006**, *128*, 9628. (b) Driess, M.; Yao, S.; Brym, M.; van Wullen, C. *Angew. Chem., Int. Ed.* **2006**, *45*, 4349. (c) Hill, N. J.; Moser, D. F.; Guzei, I. A.; West, R. *Organometallics* **2005**, *24*, 3346. (d) Fjeldberg, T.; Hope, H.; Lappert, M. F.; Power, P. P.; Thorne, A. J. *J. Chem. Soc., Chem. Commun.* **1983**, 639. (e) Olmstead, M. M.; Power, P. P. *Inorg. Chem.* **1984**, *23*, 413. (f) Tang, Y.; Felix, A. M.; Zakharov, L. N.; Rheingold, A. L.; Kemp, R. A. *Inorg. Chem.* **2004**, *43*, 7239. (g) Avent, A. G.; Drost, C.; Gehrus, B.; Hitchcock, P. B.; Lappert, M. F. *Z. Anorg. Allg. Chem.* **2004**, *630*, 2090. (h) Gans-Eichler, T.; Gudat, D.; Nieger, M. *Angew. Chem., Int. Ed.* **2002**, *41*, 1888. (i) Chorley, R. W.; Hitchcock, P. B.; Lappert, M. F.; Leung, W.-P.; Power, P. P.; Olmstead, M. M. *Inorg. Chim. Acta* **1992**, *198*, 203. (j) Braunschweig, H.; Hitchcock, P. B.; Lappert, M. F.; Pierssens, L. J.-M. *Angew. Chem., Int. Ed. Engl.* **1994**, *33*, 1156. (k) Lappert, M. F.; Slade, M. J.; Atwood, J. L.; Zaworotko, M. J. *J. Chem. Soc., Chem. Commun.* **1980**, 621. (l) Bazinet, P.; Yap, G. P. A.; Richeson, D. S. *J. Am. Chem. Soc.* **2001**, *123*, 11162. (m) Mansell, S. M.; Russell, C. A.; Wass, D. F. *Inorg. Chem.* **2008**, *47*, 11367. (n) Zabula, A. V.; Hahn, F. E.; Pape, T.; Hepp, A. *Organometallics* **2007**, *26*, 1972. (o) Hahn, F. E.; Wittenbecher, L.; LeVan, D.; Zabula, A. V. *Inorg. Chem.* **2007**, *46*, 7662. (p) Zabula, A. V.; Pape, T.; Hepp, A.; Hahn, F. E. *Organometallics* **2008**, *27*, 2756. (q) Hahn, F. E.; Zabula, A. V.; Pape, T.; Hepp, A.; Tonner, R.; Haunschild, R.; Frenking, G. *Chem.—Eur. J.* **2008**, *14*, 10716. (r) Hahn, F. E.; Heitmann, D.; Pape, T. *Eur. J. Inorg. Chem.* **2008**, 1039. (s) Charmant, J. H.; Haddow, M. F.; Hahn, F. E.; Heitmann, D.; Frölich, R.; Mansell, S. M.; Russell, C. A.; Wass, D. F. *Dalton Trans.* **2008**, 6055.

(3) Driess, M.; Janoschek, R.; Pritzkow, H.; Rell, S.; Winkler, U. *Angew. Chem., Int. Ed. Engl.* **1995**, *34*, 1614.

(4) Rivard, E.; Sutton, A. D.; Fettinger, J. C.; Power, P. P. *Inorg. Chim. Acta* **2007**, *360*, 1278.

(5) Cowley, A. H.; Giolando, D. M.; Jones, R. A.; Nunn, C. M.; Power, J. M. *Polyhedron* **1988**, *7*, 1909.

(6) Goel, S. C.; Chiang, M. Y.; Rauscher, D. J.; Buhro, W. E. *J. Am. Chem. Soc.* **1993**, *115*, 160.

(7) Druckenbrodt, C.; du Mont, W.-W.; Ruthe, F.; Jones, P. G. *Z. Anorg. Allg. Chem.* **1998**, *624*, 590.

(8) Arif, A. M.; Cowley, A. H.; Jones, R. A.; Power, J. M. *J. Chem. Soc., Chem. Commun.* **1986**, 1446.

(9) Yao, S.; Brym, M.; Merz, K.; Driess, M. *Organometallics* **2008**, *27*, 3601.

(10) For examples see: (a) Westerhausen, M.; Hausen, H.-D.; Schwarz, W. *Z. Anorg. Allg. Chem.* **1996**, *622*, 903. (b) Westerhausen, M.; Krofta, M.; Wiberg, N.; Nöth, H.; Pfitzner, A. *Z. Naturforsch. B* **1998**, *53*, 1489. (c) Westerhausen, M.; Hausen, H.-D.; Schwarz, W. *Z. Anorg. Allg. Chem.* **1995**, *621*, 877. (d) Westerhausen, M.; Krofta, M.; Schneiderbauer, S.; Piotrowski, H. *Z. Anorg. Allg. Chem.* **2005**, *631*, 1391. (e) Allan, R. E.; Beswick, M. A.; Cromhout, N. L.; Paver, M. A.; Raithby, P. R.; Trevithick, M.; Wright, D. S. *Chem. Commun.* **1996**, 1501. (f) Garcia, F.; Hahn, J. P.; McPartlin, M.; Pask, C. M.; Rothenberger, A.; Stead, M. L.; Wright, D. S. *Organometallics* **2006**, *25*, 3275.

(11) Izod, K.; McFarlane, W.; Allen, B.; Clegg, W.; Harrington, R. W. *Organometallics* **2005**, *24*, 2157.

(12) Izod, K.; Stewart, J.; Clark, E. R.; McFarlane, W.; Allen, B.; Clegg, W.; Harrington, R. W. *Organometallics* **2009**, *28*, 3327.

(13) Izod, K.; Stewart, J.; Clegg, W.; Harrington, R. W. *Organometallics* **2010**, *29*, 108.

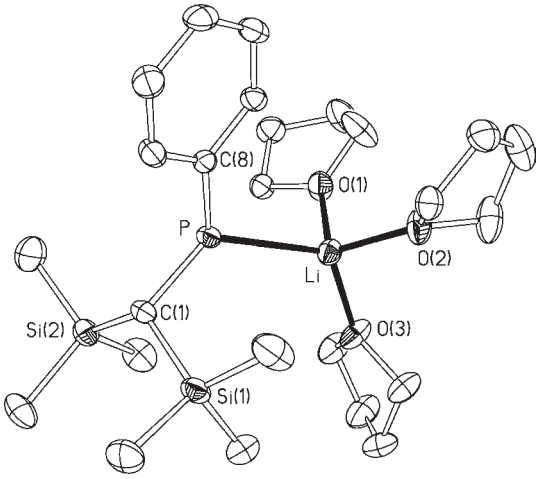

Figure 1. Molecular structure of **15**(THF) with 40% probability ellipsoids and with H atoms and minor disorder components omitted for clarity. Selected bond lengths (Å) and angles (deg): Li−P 2.551(3), Li−O(1) 1.994(3), Li−O(2) 1.936(3), Li−O(3) 1.941(3), P−C(1) 1.8913(16), P−C(8) 1.7985(17), C(1)−Si(1) 1.8729(17), C(1)−Si(2) 1.8643(16), P−Li−O(1) 102.43(12), P−Li−O(2) 118.08(13), P−Li−O(3) 124.01(14), O(1)−Li−O(2) 106.15(15), O(1)−Li−O(3) 101.23(14), O(2)−Li−O(3) 102.49(14).

Scheme 1. [R = $(Me_3Si)_2CH$]

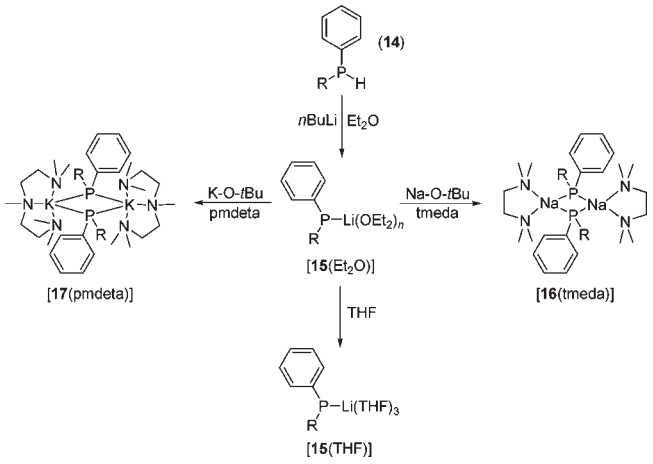

rise to two signals in the ^{1}H spectrum, the $SiMe_3$ groups in **15**(THF), **16**(tmeda), and **17**(pmdeta) are equivalent on the NMR time-scale because of rapid intermolecular exchange via P-M cleavage and re-coordination.

Compound **15**(THF) crystallizes as discrete monomers in which the lithium ion is coordinated by the phosphorus atom of the phosphanide ligand and the oxygen atoms of three molecules of THF in a distorted tetrahedral geometry. The molecular structure of **15**(THF) is shown in Figure 1, along with selected bond lengths and angles. The Li−P distance of 2.551(3) Å is typical of such contacts,[14a] and is similar to the corresponding distances in the closely related compounds $[(2,4,6\text{-}Me_3C_6H_2)PH]Li(THF)_3$ [2.533(9) Å],[14b] $[\{(Me_3Si)_2CH\}(C_6H_4\text{-}2\text{-}CH_2NMe_2)P]Li(THF)_2$ [2.535(8) and 2.535(7) Å][14c] and $[\{(Me_3Si)_2CH\}(C_6H_4\text{-}2\text{-}NMe_2)P]Li(THF)_2$ [2.498(5) and 2.505(5) Å][15] and in other lithium phosphanides; for example,

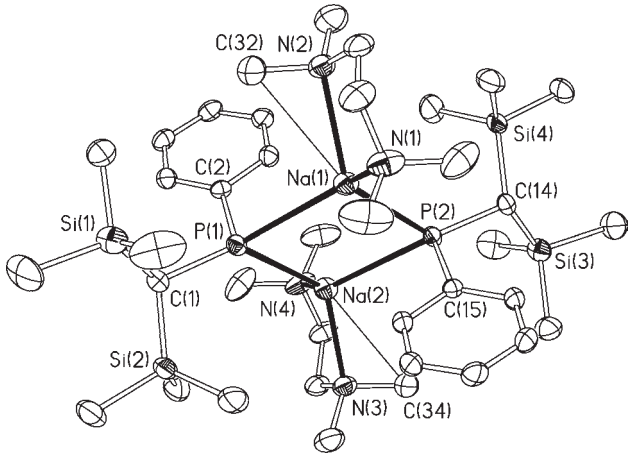

Figure 2. Molecular structure of **16**(tmeda) with 40% probability ellipsoids and with H atoms omitted for clarity. Selected bond lengths (Å) and angles (deg): Na(1)−P(1) 2.9701(9), Na(1)−P(2) 2.9627(9), Na(2)−P(1) 2.9386(9), Na(2)−P(2) 2.9341(9), Na(1)−N(1) 2.4868(18), Na(1)−N(2) 2.5169(18), Na(2)−N(3) 2.4921(18), Na(2)−N(4) 2.4712(18), Na(1)···C(32) 3.100(3), Na(2)···C(34) 3.125(3), Na(1)−P(1)−Na(2) 84.71(2), Na(1)−P(2)−Na(2) 84.92(2), P(1)−Na(1)−P(2) 94.52(2), P(1)−Na(2)−P(2) 95.79(2), N(1)−Na(1)−N(2) 74.65(6), N(3)−Na(2)−N(4) 74.94(6).

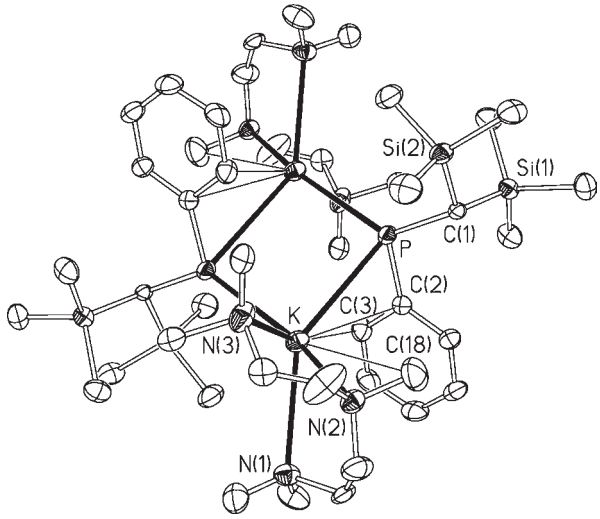

Figure 3. Molecular structure of **17**(pmdeta) with 40% probability ellipsoids and with H atoms and minor disorder components omitted for clarity. Selected bond lengths (Å) and angles (deg): K−P 3.4862(15), K−P′ 3.3351(12), K−N(1) 3.053(3), K−N(2) 2.905(3), K−N(3) 2.874(3), K−C(2) 3.222(3), K−C(3) 3.162(3), K···C(18) 3.445(4), P−C(1) 1.893(3), P−C(2) 1.809(3), C(1)−Si(1) 1.884(3), C(1)−Si(2) 1.880(3), P−K−P′ 81.47(3), K−P−K′ 98.53(3), N(1)−K-N(2) 61.29(8), N(2)−K-N(3) 62.99(8). A prime indicates an inversion-generated atom.

the Li−P distances in $[(Ph_2P)Li(DME)]_\infty$ are 2.563(3) and 2.541(3) Å.[16]

Compounds **16**(tmeda) and **17**(pmdeta) crystallize as dimers containing rhombus-shaped P_2M_2 cores. The molecular structures of **16**(tmeda) and **17**(pmdeta) are shown in Figures 2 and 3, respectively, along with selected bond lengths and angles. In **16**(tmeda) each sodium ion is coordinated by the P atoms of two phosphanide ligands and the N atoms of a molecule of tmeda to give a four-coordinate distorted tetrahedral metal center; in addition

(14) (a) Izod, K. *Adv. Inorg. Chem.* **2000**, *50*, 33. (b) Bartlett, R. A.; Olmstead, M. M.; Power, P. P.; Sigel, G. A. *Inorg. Chem.* **1987**, *26*, 1941. (c) Clegg, W.; Doherty, S.; Izod, K.; Kagerer, H.; O'Shaughnessy, P.; Sheffield, J. M. *J. Chem. Soc., Dalton Trans.* **1999**, 1825.

(15) Izod, K.; Stewart, J. C.; Clegg, W.; Harrington, R. W. *Dalton Trans.* **2007**, 257.

(16) Steiglitz, G.; Neumüller, B.; Dehnicke, K. *Z. Naturforsch. B* **1993**, *48*, 156.

Scheme 2. [R = $(Me_3Si)_2CH$]

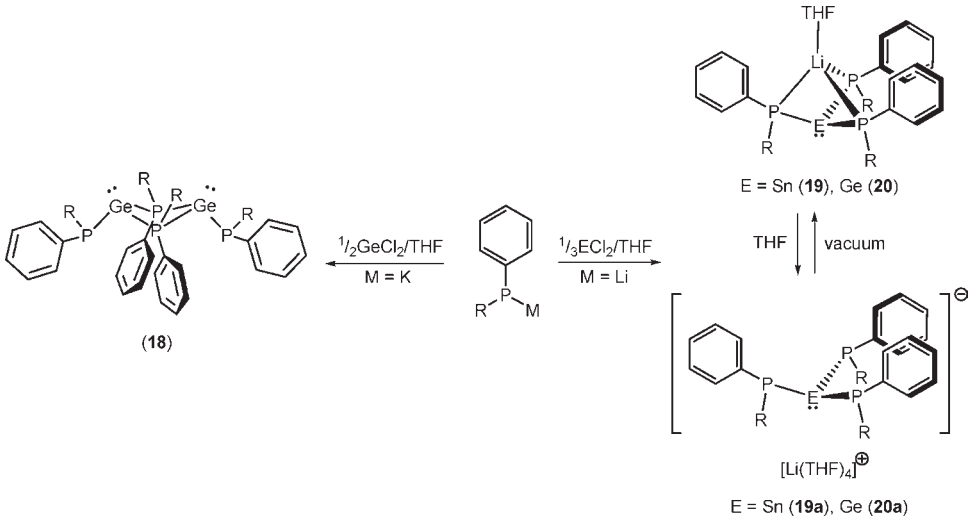

there are short contacts between each sodium ion and one of the methyl groups from the adjacent tmeda ligand [Na(1)···C(23) 3.100(3), Na(2)···C(34) 3.125(3) Å]. The dimeric molecule of **16**(tmeda) has no crystallographically imposed symmetry, but is essentially centrosymmetric; the P−Na distances lie in the range 2.9341(9)−2.9701(9) Å and are somewhat longer than the corresponding distances in the monomeric compounds [{$(Me_3Si)_2CH$}(C_6H_4-2-CH_2NMe_2)P]Na(tmeda) [2.8189(8) Å][14c] and [{$(Me_3Si)_2CH$}(C_6H_4-2-NMe_2)P]Na(tmeda) [2.8396(9) Å],[15] but are similar to the Na−P distances in the phosphanide-bridged dimer [{(C_6H_4-2-OMe)$_2$P}Na(diglyme)]$_2$ [2.861(2)−3.047(2) Å].[17] Each potassium ion in **17**(pmdeta) is coordinated by the phosphorus atoms of two phosphanide ligands and by the three N atoms of a molecule of pmdeta, affording a five-coordinate metal center; in addition, there are short contacts between each potassium ion and two of the carbon atoms in the phenyl ring of one phosphanide ligand [K−C(2) 3.222(3), K−C(3) 3.162(3) Å] and between each potassium and the central methyl group of the pmdeta ligand [K···C(18) 3.445(4) Å]. The P−K distances in the strictly centrosymmetric dimer of **17**(pmdeta) [3.4862(15) and 3.3351(12) Å] are somewhat longer than the P−K distances in monomeric [{$(Me_3Si)_2CH$}(C_6H_4-2-CH_2NMe_2)P]K(pmdeta) [3.2326(6) Å][14c] and [{$(Me_3Si)_2CH$}(C_6H_4-2-NMe_2)P]K-(pmdeta) [3.2198(10) Å],[15] but are similar to the P−K distances in a range of potassium phosphanide complexes containing μ_2-briding phosphanide ligands; for example, the P−K distances in polymeric [{$(Me_3Si)_2P$}K(THF)]$_n$ are 3.3169(7), 3.4063(8), and 3.4272(8) Å.[18] In both **16**-(tmeda) and **17**(pmdeta) the phosphanide ligands adopt an *anti* arrangement, which minimizes steric interactions between the bulky $(Me_3Si)_2CH$ groups.

The reaction between $GeCl_2$(1,4-dioxane) and 2 equiv of **17** in THF yields the phosphagermylene [[{$(Me_3Si)_2CH$}-(Ph)P]$_2$Ge]$_2$ (**18**), after a simple workup, as a sticky, orange-brown solid, which may be crystallized from cold hexamethyldisiloxane containing a few drops of diethyl ether as orange blocks of the solvate [[{$(Me_3Si)_2CH$}(Ph)P]$_2$Ge]$_2$·Et_2O (**18**·Et_2O) suitable for X-ray crystallography (Scheme 2). Compound **18**·Et_2O crystallizes with two independent molecules of **18** in the asymmetric unit with opposite $P^t_R P^t_R$ and $P^t_S P^t_S$ stereochemistry (where P^t and P^{br} refer to the terminal and bridging phosphorus atoms, respectively (see below)), which differ only trivially in their bond lengths and angles, along with two molecules of diethyl ether; for brevity, the following discussion relates to molecule 1. The structure of molecule 1 of **18** is shown in Figure 4, along with selected bond lengths and angles. Although the structure is racemic, this is not a necessary consequence of the space group symmetry, which could equally well support an enantiopure structure, for example, by spontaneous resolution on crystallization.

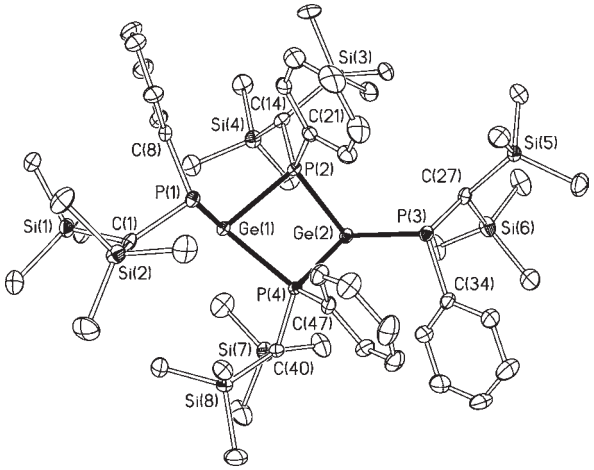

Figure 4. Molecular structure of one of the two independent molecules of **18**·Et_2O with 40% probability ellipsoids; H atoms and solvent of crystallization omitted for clarity. Selected bond lengths (Å) and angles (deg) for the independent molecule shown: Ge(1)−P(1) 2.4151(13), Ge-(1)−P(2) 2.4362(13), Ge(1)−P(4) 2.4361(12), Ge(2)−P(2) 2.4442(12), Ge(2)−P(3) 2.4153(13), Ge(2)−P(4) 2.4369(13), Ge(1)−P(2)−Ge(2) 90.78(4), Ge(1)−P(4)−Ge(2) 90.95(4), P(1)−Ge(1)−P(2) 96.86(4), P-(1)−Ge(1)−P(4) 107.65(4), P(2)−Ge(1)−P(4) 80.62(4), P(3)−Ge(2)−P-(2) 104.89(4), P(3)−Ge(2)−P(4) 99.54(4), P(2)−Ge(2)−P(4) 80.44(4).

The solvent of crystallization in **18**·Et_2O is only weakly held, and ^{1}H NMR spectra obtained from crystalline samples which had been exposed to vacuum for a few minutes exhibited signals due to sub-stoichiometric amounts of diethyl ether. Similarly, a sample of **18**·Et_2O which had been

(17) Aspinall, H. C.; Tillotson, M. R. *Inorg. Chem.* **1996**, *35*, 5.
(18) Englich, U.; Hassler, K.; Ruhlandt-Senge, K.; Uhlig, F. *Inorg. Chem.* **1998**, *37*, 3532.

exposed to vacuum for 15 min had an elemental (C and H) composition corresponding to the dimer with no solvent of crystallization.

Compound **18**·Et_2O crystallizes as discrete dimers in which two phosphanide ligands bridge in a μ_2-fashion between the two germanium centers, generating a butterfly shaped Ge_2P_2 core. The Ge−P^{br} distances within this core range from 2.4361(12) to 2.4442(12) Å and compare with Ge−P distances of 2.4261(11) and 2.4217(11) Å in the Ge_2P_2 core of **6**.[7] The Ge−P^t distances in **18**·Et_2O of 2.4151(13) and 2.4153(13) Å are slightly shorter than the Ge−P^{br} distances but are similar to the Ge−P distances in **10** [2.4023(4) and 2.4114(4) Å].[11] The germanium centers possess a stereochemically active lone pair and adopt a trigonal pyramidal geometry [sum of angles at Ge(1) 285.14, Ge(2) 284.87°].

The dimers crystallize with a *syn*, *syn*-arrangement, in which the two terminal phosphanides lie on the same side of the P_2Ge_2 core and the bridging phosphanide ligands are arranged such that the bulky $(Me_3Si)_2CH$ groups lie on the same side of the P_2Ge_2 core. This arrangement enables the planar phenyl substituents of the bridging ligands to adopt a configuration which minimizes steric interactions with the bulky $(Me_3Si)_2CH$ substituents of the terminal phosphanide ligands and positions the bulky $(Me_3Si)_2CH$ substituents of the bridging ligands on the opposite side of the P_2Ge_2 core to the terminal phosphanide ligands. Steric interactions between the terminal phosphanide ligands are minimized by a puckering of the P_2Ge_2 core (the angle between the P(2)−Ge(1)−P(4) and P(2)−Ge(2)−P(4) planes is 138.0°). This configuration contrasts with the configuration adopted by the closely related dimer **6**, in which the terminal phosphanide ligands are positioned *anti* to one another.[7] The difference between the configurations of **18**·Et_2O and **6** may be attributed to the steric properties of the unsymmetrical bridging ligands in the former, which favor the *syn*, *syn* arrangement, whereas the symmetrical bridging ligands in the latter do not influence the arrangement of the terminal ligands and so these adopt a configuration which minimizes terminal-terminal ligand interactions.

The dimeric structure of **18** appears to remain intact in solution, even in the donor solvent THF. The $^{31}P\{^1H\}$ NMR spectrum of **18** in d_8-THF consists of a dominant pair of triplets at −58.1 (**A**) and −37.3 ppm (**B**) (J_{PP} = 17.4 Hz), consistent with the dimeric structure observed in the solid state. In addition, small poorly resolved triplets are observed at −50.5 (**C**), −43.3 (**D**), −36.7 (**E**), and −26.4 ppm (**F**) with approximately 10% relative intensity compared to the major signals **A** and **B**. A $^{31}P-^{31}P$ COSY spectrum shows correlations between the pairs of peaks **A** and **B**, **C** and **F**, and **D** and **E**, suggesting that the low intensity signals may be assigned to two additional dimeric species. However, variable temperature ^1H, $^{31}P\{^1H\}$ and $^{31}P-^{31}P$ EXSY NMR experiments reveal that the three species present in solution are not undergoing exchange; the ^1H and $^{31}P\{^1H\}$ NMR spectra of **18** in d_8-THF are invariant over the temperature range −50 to 50 °C. The formation of three independent dimeric species in solution is supported by the NMR spectra of batches of **18** from different preparations, which show different proportions of the minor components, although these minor components always comprise < 10% of the total product. While it is not possible to unambiguously attribute these minor signals to specific species, it is likely that one of the low concentration dimeric species is the alternative $P^t_R P^t_S$ diastereomer of **18**.

Given the similar steric properties of the ligands in **10** and **18**·Et_2O it is clear that, in the absence of intramolecular coordination of the Ge center by a peripheral amino substituent, the germanium center remains sufficiently Lewis acidic that dimerization occurs. In such systems the electron deficiency of Ge(II) or Sn(II) centers may alternatively be alleviated through the formation of ate complexes. In this regard, we find that treatment of $SnCl_2$ with 2 equiv of **15** in THF preferentially yields the ate complex $[\{(Me_3Si)_2CH\}(Ph)P]_3SnLi(THF)$ (**19**), rather than the expected homoleptic complex $[\{(Me_3Si)_2CH\}(Ph)P]_2Sn$. Repeated experiments reveal that complex **19** is formed irrespective of the ratio of $SnCl_2$:**15** employed or the conditions used; presumably the LiCl side product is contaminated in these cases with unreacted $SnCl_2$. In contrast, the reaction between 2 equiv of the potassium salt **17** and $SnCl_2$ results in the formation of the diphosphane $\{(Me_3Si)_2CH\}(Ph)P-P(Ph)\{CH(SiMe_3)_2\}$ and elemental tin; we have previously observed similar behavior in the reactions of $SnCl_2$ or $PbCl_2$ with other potassium phosphanides.[19]

Rational synthesis of **19** may be achieved through the reaction between $SnCl_2$ and 3 equiv of **15**; this gives **19** in good yield as orange crystals, after recrystallization from methylcyclohexane. Similarly, we find that treatment of $GeCl_2$(1,4-dioxane) with 3 equiv of **15** gives the corresponding ate complex $[\{(Me_3Si)_2CH\}(Ph)P]_3GeLi(THF)$ (**20**) in good yield. Unfortunately, we were unable to obtain single crystals of **19** suitable for X-ray crystallography; however, elemental analyses and NMR spectroscopy unambiguously confirm the identity of this compound (see below). In contrast, single crystals of the germanium analogue **20** suitable for X-ray crystallography were obtained from cold *n*-hexane/THF.

Compound **20** is chiral at each of the phosphorus centers and crystallizes as discrete cage-like molecules; the crystal studied contains the $P_RP_RP_R$ stereoisomer and its $P_SP_SP_S$ enantiomer, since the structure, with glide planes, is noncentrosymmetric, but achiral. The molecular structure of **20** is shown in Figure 5, along with selected bond lengths and angles; 3-fold disorder of the whole molecule about the Ge−Li axis was reasonably modeled by inclusion of a minor component of all three P atoms, disorder of the hydrocarbon substituents remaining unresolved. The three phosphorus atoms of the phosphanide ligands form μ_2-bridges between the germanium and lithium centers to give a trigonal bipyramidal GeP_3Li core, affording a trigonal pyramidal geometry at the germanium center. The coordination sphere of the lithium ion is completed by a molecule of THF, giving the lithium ion a distorted tetrahedral geometry. The Ge−P distances of 2.4609(18), 2.4449(19), and 2.4497(19) Å (taking only the major disorder component) lie between the Ge−P^{br} distances in **6** [2.4261(11) and 2.4217(11) Å][7] and the Ge−P^{br} distances in the heteroleptic phosphanide-bridged dimer **9** [2.4876(8) and 2.4926(8) Å].[7] The Li−P distances of 2.663(9), 2.591(10), and 2.593(10) Å are typical of such contacts; for example, the Li−P distances in the phosphanide-bridged dimer $[(Ph_2P)Li(tmeda)]_2$ range from 2.574(19) to 2.629(20) Å.[20] The P−Ge−P angles in **20** lie in

(19) Blair, S.; Izod, K.; Taylor, R.; Clegg, W. *J. Organomet. Chem.* **2002**, *656*, 43.
(20) Mulvey, R. E.; Wade, K.; Armstrong, D. R.; Walker, G. T.; Snaith, R.; Clegg, W.; Reed, D. *Polyhedron* **1987**, *6*, 987.

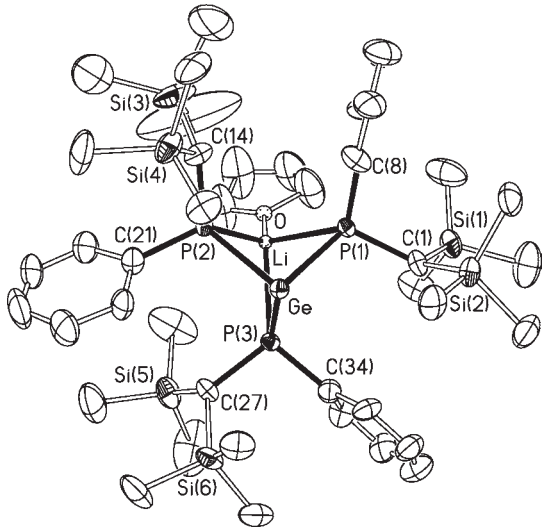

Figure 5. Molecular structure of **20** with 40% probability ellipsoids and with H atoms and minor disorder components omitted for clarity. Selected bond lengths (Å) and angles (deg): Ge−P(1) 2.4609(18), Ge−P(2) 2.4449(19), Ge−P(3) 2.4497(19), Li−P(1) 2.663(9), Li−P(2) 2.591(10), Li−P(3) 2.593(10), Li−O 1.955(9), Ge−P(1)−Li 80.82(19), Ge−P(2)−Li 82.6(2), Ge−P(3)−Li 82.5(2), P(1)−Ge-P(2) 85.11(6), P(1)−Ge-P(3) 84.82(6), P(2)−Ge-P(3) 84.54(6), P(1)−Li-P(2) 78.3(2), P(1)−Li-P(3) 78.1(2), P(2)−Li-P(3) 78.9(2), P(1)−Li−O 127.8(4), P(2)−Li−O 134.9(5), P(3)−Li−O 136.2(5).

Chart 2. [R = $(Me_3Si)_2CH$]

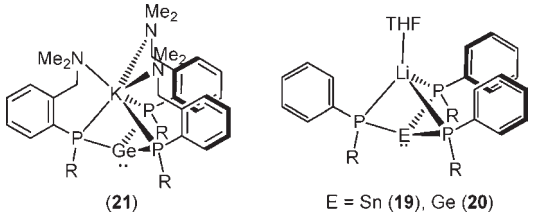

Scheme 3

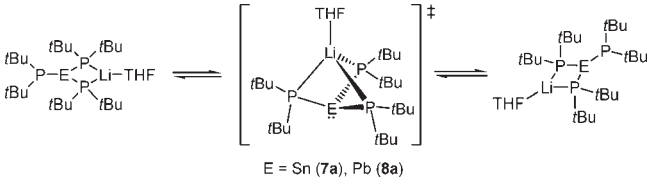

the small range 84.54(6) to 85.11(6)°, while the P−Li−P angles fall in the range 78.1(2) to 78.9(2)°.

The molecular structure of **20** closely resembles that of the ate complex $[\{(Me_3Si)_2CH\}(C_6H_4\text{-}2\text{-}CH_2NMe_2)P]_3GeK$ (**21**),[11] which we reported previously, but which has additional N-donor groups that bind the potassium ion (Chart 2); this compound contains a GeP_3K core similar to the GeP_3Li core observed in **20**. However, the structure of **20** differs markedly from that of the ate complexes $(tBu_2P)E(\mu_2\text{-}tBu_2P)_2Li(THF)$ [E = Sn (**7**), Pb (**8**)],[8] in which only two phosphanide ligands bridge between the lithium and group 14 element centers. It is notable, however, that Cowley, Jones, and co-workers propose a transition state of the form $E(\mu_2\text{-}tBu_2P)_3Li(THF)$ (**7a**/**8a**), in which all three phosphanide ligands bridge the lithium and tin (or lead) atoms, to account for the rapid dynamic equilibrium between the bridging and terminal phosphanides in these

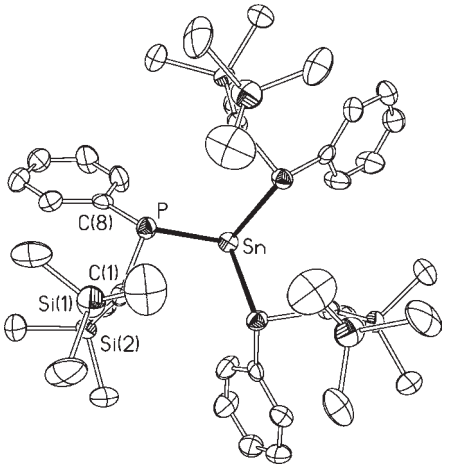

Figure 6. Structure of the anion of **19a** with 40% probability ellipsoids and with H atoms omitted for clarity. Selected bond lengths (Å) and angles (deg): Sn−P 2.649(2), P−C(1) 1.905(7), P−C(8) 1.849(7), Li−O(1) 1.929(11), Li−O(2) 1.94(3), P−Sn−P′ 91.41(6), O(1)−Li−O(2) 110.8(7), O(1)−Li−O(1′) 108.1(8). The prime denotes a symmetry-generated atom.

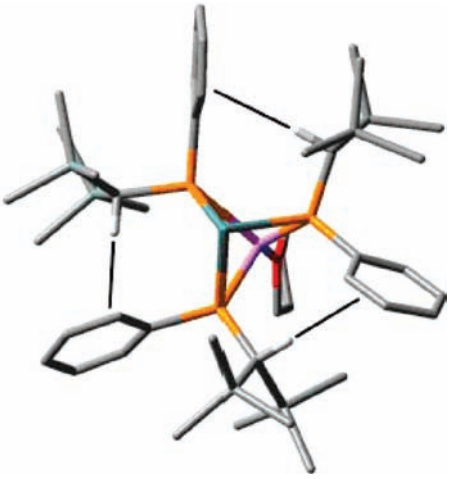

Figure 7. Proximity of the methine H atoms to the adjacent aromatic rings in **19** and **20**.

latter compounds (Scheme 3). This transition state clearly bears a strong resemblance to **20**.

Although we were unable to obtain single crystals of the tin analogue of **20**, recrystallization of **19** from cold methylcyclohexane/THF gives single crystals of the solvent-separated ion pair $[[\{(Me_3Si)_2CH\}(Ph)P]_3Sn][Li(THF)_4]$ (**19a**) suitable for X-ray crystallography. The molecular structure of the anion of **19a** is shown in Figure 6, along with selected bond lengths and angles; the structure of the cation is unexceptional and is not shown. Compound **19a** crystallizes in the noncentrosymmetric cubic space group $I\bar{4}3c$ as a separated ion pair consisting of an anion containing a tin atom coordinated by three phosphanide ligands, in a trigonal pyramidal geometry, and a cation containing a lithium ion coordinated by four molecules of THF in a distorted tetrahedral geometry. The cation and anion have exact, crystallographic, C_3 symmetry; the cation is therefore subject to 3-fold disorder about the Li−O(2) axis. Each phosphanide ligand is chiral, and the crystal studied was of the $P_SP_SP_S$ and $P_RP_RP_R$ stereoisomers, the structure being racemic as a result of $\bar{4}$ improper rotation axes and glide planes. The Sn−P distance of 2.649(2) Å is

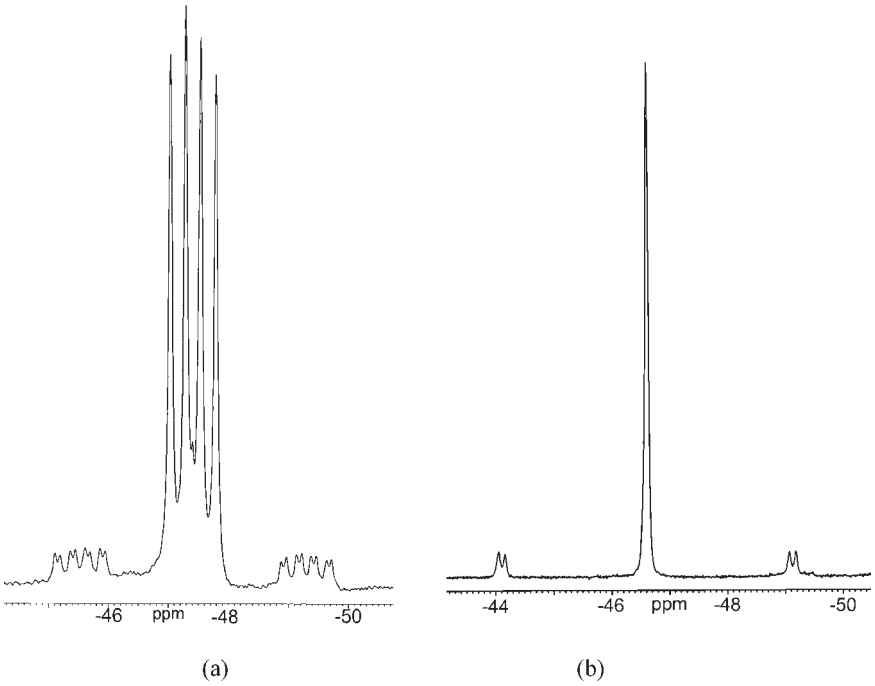

Figure 8. $^{31}P\{^{1}H\}$ NMR spectra of **19** in (a) d_8-toluene and (b) d_8-THF.

somewhat longer than the corresponding distance in the monomeric diphosphastannylene **2** [average Sn−P 2.567(1) Å], but is similar to the Sn−P distances in the ate complex **7** [2.684(4), 2.702(3), and 2.671(4) Å]. In spite of the increased size of Sn compared to Ge, the P−Sn−P angle of 91.41(6)° is substantially wider than the P−Ge−P angle in **20** [84.82(6)−85.11(6)°], consistent with the constraints associated with the formation of a contact ion pair in the latter compound. Although voids of about 1000 Å^3 can be identified in the crystal structure, the SQUEEZE procedure of PLATON finds little electron density in them and gives only a minor reduction in *R* factor, so any solvent must be only loosely held and is largely lost, even in the brief handling and transfer of a crystal from the mother liquor to the cold gas stream of the diffractometer. The original, rather than SQUEEZE-generated, data have been used for the results reported here.

The $^{31}P\{^{1}H\}$ NMR spectrum of **20** in d_8-toluene consists of a 1:1:1:1 quartet at −32.2 ppm because of coupling to a single ^{7}Li nucleus (J_{PLi} = 50.0 Hz); the $^{7}Li\{^{1}H\}$ spectrum consists of a binomial quartet at 3.18 ppm. These spectra clearly suggest that the cage-like structure observed in the solid state persists in non-donor solvents. Consistent with this, the ^{1}H NMR spectrum of **20** exhibits a singlet at −1.32 ppm because of the methine proton of the phosphanide ligand, two equal intensity singlets at 0.04 and 0.17 ppm, because of the diastereotopic $SiMe_3$ groups, along with signals due to the phenyl rings and THF. The unusually high-field chemical shift of the methine proton of the phosphanide ligand may be attributed to chemical shift anisotropy associated with the presence of a nearby aromatic ring. Examination of the solid state structure of **20** clearly shows that the position of the methine proton of each phosphanide ligand is fixed directly over the face of the phenyl ring of an adjacent ligand, and so these protons experience an upfield shift due to a substantial ring current effect (Figure 7).

The $^{31}P\{^{1}H\}$ NMR spectrum of **19** consists of a 1:1:1:1 quartet at 47.3 ppm (J_{PLi} = 50.9 Hz), with well-resolved satellites due to coupling to $^{117}Sn/^{119}Sn$ (J_{PSn} = 747 and 780 Hz) (Figure 8a), while the $^{7}Li\{^{1}H\}$ spectrum consists of a binomial quartet at 3.4 ppm; the $^{119}Sn\{^{1}H\}$ spectrum consists of a binomial quartet centered at −105 ppm (J_{PSn} = 780 Hz). As was observed for **20**, in the ^{1}H NMR spectrum of **19** the methine protons exhibit an unusual high field chemical shift of −1.16 ppm because of the proximity of these protons to the face of the adjacent aromatic rings. These spectra are clearly consistent with the presence in solution of a cage-like ate complex having a SnP_3Li core similar to the GeP_3Li core observed in the solid state structure of **20**.

Exposure of the separated ion pair complex **19a** to vacuum for short periods leads to loss of THF and complete conversion to the cage-like form **19**, as established by elemental analyses and NMR spectroscopy. However, NMR spectra consistent with the separated ion pair form **19a** may be obtained from solutions of **19** in d_8-THF. The $^{31}P\{^{1}H\}$ NMR spectrum of **19** in d_8-THF (Figure 8b) consists of a singlet at −46.6 ppm exhibiting well-resolved satellites due to coupling to $^{117}Sn/^{119}Sn$ (J_{PSn} = 995 and 1038 Hz); the $^{7}Li\{^{1}H\}$ NMR spectrum of **19** in this solvent consists of a singlet at 2.3 ppm and the $^{119}Sn\{^{1}H\}$ NMR spectrum consists of a binomial quartet at 62 ppm (J_{PSn} = 1038 Hz). The lack of $^{31}P-^{7}Li$ coupling and the large downfield shift of the ^{119}Sn signal are consistent with the presence of separated ion pairs in this solvent. Similarly, the $^{31}P\{^{1}H\}$ and $^{7}Li\{^{1}H\}$ NMR spectra of **20** in d_8-THF consist of singlets at −42.3 and 2.5 ppm, respectively, consistent with the presence of a separated ion pair species $[[\{(Me_3Si)_2CH\}(Ph)P]_3Ge][Li(THF)_4]$ (**20a**). Removal of solvent in vacuo from THF solutions of **20a** results in complete conversion to the contact ion pair form **20**.

For both **19a** and **20a** the ^{1}H NMR spectra are as expected. The methine protons give rise to signals at 1.04 and 0.68 ppm, respectively; free rotation about the P−E bond on removal of the "capping" lithium ion in each case has the result that these protons are no longer constrained to lie over an adjacent

aromatic ring and so no longer experience any significant chemical shift anisotropy.

Conclusions

The sterically demanding secondary phosphane $\{(Me_3Si)_2CH\}(Ph)PH$ (**14**), which lacks a peripheral donor group, is readily accessible and undergoes deprotonation on treatment with *n*-BuLi to give the monomeric phosphanide $[\{(Me_3Si)_2CH\}(Ph)P]Li(THF)_3$ [**15**(THF)], after crystallization. The dimeric sodium and potassium derivatives $[[\{(Me_3Si)_2CH\}(Ph)P]Na(tmeda)]_2$ [**16**(tmeda)] and $[[\{(Me_3Si)_2CH\}(Ph)P]K(pmdeta)]_2$ [**17**(pmdeta)] may also be obtained in good yields after crystallization in the presence of the corresponding tertiary amine.

Whereas reactions between $GeCl_2$(1,4-dioxane) and either of the donor-functionalized compounds $[\{(Me_3Si)_2CH\}(C_6H_4\text{-}2\text{-}NMe_2)P]K$ or $[\{(Me_3Si)_2CH\}(C_6H_4\text{-}2\text{-}CH_2NMe_2)P]K$ yield the corresponding monomeric, base-stabilized diphosphagermylenes $[\{(Me_3Si)_2CH\}(C_6H_4\text{-}2\text{-}(CH_2)_nNMe_2)P]_2Ge$ [n = 0 (**12**), 1 (**10**)], the corresponding reaction between 2 equiv of **17**(Et_2O) and $GeCl_2$(1,4-dioxane) yields the dimeric complex $[[\{(Me_3Si)_2CH\}(Ph)P]_2Ge]_2.Et_2O$ (**18**·Et_2O). This clearly demonstrates that, in the absence of peripheral donor functionalization, the steric demands of these ligands are insufficient to prevent oligomerization.

Unexpectedly, the reaction between $SnCl_2$ and the lithium complex **15**(Et_2O) yields the ate complex $[\{(Me_3Si)_2CH\}(Ph)P]_3SnLi(THF)$ (**19**), irrespective of the reaction stoichiometry. This compound and its germanium analogue (**20**) retains its structure in toluene solution, but forms the separated ion pair complex $[[\{(Me_3Si)_2CH\}(Ph)P]_3Sn][Li(THF)_4]$ (**19a**) on crystallization from *n*-hexane/THF.

Experimental Section

All manipulations were carried out using standard Schlenk techniques under an atmosphere of dry nitrogen. Diethyl ether, THF, *n*-hexane, methylcyclohexane, and light petroleum (bp 40−60 °C) were dried prior to use by distillation under nitrogen from sodium, potassium, or sodium/potassium alloy; hexamethyldisiloxane was dried by distillation under nitrogen from calcium hydride. THF and hexamethyldisiloxane were stored over activated 4A molecular sieves; diethyl ether, *n*-hexane, methylcyclohexane and light petroleum were stored over a potassium film. Deuterated toluene and THF were distilled from potassium and deoxygenated by three freeze−pump−thaw cycles and were stored over activated 4A molecular sieves. Germanium(II) chloride was prepared as its 1,4-dioxane adduct by a previously published procedure;[21] $[(Me_3Si)_2CH]Li$ was prepared as previously described.[22] Tin(II) chloride was dried with chlorotrimethylsilane prior to use; potassium *tert*-butoxide and sodium *tert*-butoxide were dried under vacuum at 100 °C/10^{-2} mmHg for 3 h before use. All other compounds were used as supplied by the manufacturer.

^1H and $^{13}C\{^1H\}$ NMR spectra were recorded on a JEOL ECS500 spectrometer operating at 500.16 and 125.65 MHz, respectively, or a Bruker Avance300 spectrometer operating at 300.15 and 75.47 MHz, respectively; chemical shifts are quoted in parts per million (ppm) relative to tetramethylsilane. $^{31}P\{^1H\}$, $^7Li\{^1H\}$, and $^{119}Sn\{^1H\}$ NMR spectra were recorded on a JEOL ECS500 spectrometer operating at 202.35, 194.38, and 186.50 MHz, respectively; chemical shifts are quoted in ppm relative to external 85% H_3PO_4, external 0.1 M LiCl, and external Me_4Sn, respectively. Elemental analyses were obtained by the Elemental Analysis Service of London Metropolitan University.

$\{(Me_3Si)_2CH\}(Ph)PH$ (14). A solution of $[(Me_3Si)_2CH]Li$ (3.56 g, 21.4 mmol) in diethyl ether (30 mL) was added, dropwise, to a cold (−78 °C) solution of $PhPCl_2$ (3.83 g, 21.4 mmol) in diethyl ether (20 mL). The reaction mixture was allowed to warm to room temperature and was stirred for 2 h. The solvent was removed in vacuo giving a white solid, which was redissolved in THF (30 mL). Solid $LiAlH_4$ (0.81 g, 21.4 mmol) was cautiously added, and the reaction mixture was heated under reflux for 2 h. The reaction mixture was allowed to cool to room temperature, and excess $LiAlH_4$ was quenched by the careful addition of deoxygenated water (30 mL). The organic layer was decanted, and the aqueous layer was extracted into diethyl ether (3 × 20 mL). The combined organic extracts were dried over 4A molecular sieves, the solution was filtered, and the solvent was removed in vacuo from the filtrate to give **14** as a colorless oil. Yield: 3.72 g, 64.9%. ^1H NMR ($CDCl_3$, 294 K): δ 0.07 (s, 9H, $SiMe_3$), 0.15 (s, 9H, $SiMe_3$), 0.47 (m, 1H, CHP), 4.37 (dd, $^3J_{HH}$ = 5.0 Hz, J_{PH} = 205.4 Hz, 1H, PH), 7.30−7.55 (m, 5H, Ph). $^{13}C\{^1H\}$ NMR ($CDCl_3$, 294 K): δ 0.02 ($SiMe_3$), 7.24 (d, J_{PC} = 42.3 Hz, CHP), 127.37, 127.53 (Ph), 132.92 (d, J_{PC} = 17.7 Hz, Ph), 138.04 (d, J_{PC} = 16.3 Hz, Ph). ^{31}P NMR ($CDCl_3$, 294 K): δ −60.2 (d, J_{PH} = 205.4 Hz).

$[[\{(Me_3Si)_2CH\}(Ph)P]Li(THF)_3]$ [15(THF)]. To a stirred solution of **14** (0.92 g, 3.43 mmol) in diethyl ether (20 mL) was added *n*-BuLi (1.37 mL, 3.43 mmol), and this mixture was stirred at room temperature for 1 h. The solvent was removed in vacuo giving an orange, viscous oil which was crystallized from cold (−30 °C) *n*-hexane containing a few drops of THF as yellow blocks of **15**(THF) suitable for X-ray crystallography. Yield: 1.32 g, 78.4%. Anal. Calcd. for $C_{25}H_{48}LiO_3PSi_2$: C, 61.13; H, 9.78%. Found: C, 60.95; H, 9.58%. ^1H NMR (C_6D_6, 296 K): δ 0.38 (s, 18H, $SiMe_3$), 0.64 (s, 1H, CHP), 1.27 (m, 12H, THF), 3.45 (m, 12H, THF), 6.72−7.53 (m, 5H, Ph). $^{13}C\{^1H\}$ NMR (C_6D_6, 296 K): δ 1.48 ($SiMe_3$), 2.55 (d, J_{PC} = 52.8 Hz, CHP), 25.15 (THF), 68.12 (THF), 117.85(Ph), 126.16 (d, J_{PC} = 17.3 Hz, Ph), 133.77 (d, J_{PC} = 17.3 Hz, Ph), 157.73 (d, J_{PC} = 45.1 Hz, Ph). $^{31}P\{^1H\}$ NMR (C_6D_6, 296 K): δ −77.3.

$[[\{(Me_3Si)_2CH\}(Ph)P]Na(tmeda)]_2$ [16(tmeda)]. To a solution of **14** (1.23 g, 4.60 mmol) in diethyl ether (20 mL) was added *n*-BuLi (1.84 mL, 4.60 mmol), and this mixture was stirred for 1 h. The resulting solution was added to a slurry of NaO-*t*-Bu (0.44 g, 4.60 mmol) in diethyl ether (20 mL), and this mixture was stirred at room temperature for 1 h. The solvent was removed in vacuo giving a sticky yellow solid which was washed with light petroleum (3 × 20 mL) and dried in vacuo, yielding a yellow, pyrophoric solid (**16**). Crystals of the adduct **16**(tmeda) suitable for an X-ray crystallographic study were obtained from cold (−30 °C) methylcyclohexane containing 1 equiv of tmeda. Yield: 1.01 g, 54.2%. Anal. Calcd. for $C_{19}H_{40}NaN_2PSi_2$: C, 56.07; H, 9.84; N, 6.89%. Found: C, 55.90; H, 9.75; N, 6.72%. ^1H NMR (d_8-THF, 296 K): δ 0.20 (s, 18H, $SiMe_3$), 0.30 (s, 1H, CHP), 2.18 (s, 12H, NMe_2), 2.35 (s, 4H, CH_2N), 6.28−7.29 (m, 5H, Ph). $^{13}C\{^1H\}$ NMR (d_8-THF, 296 K): δ 0.89 ($SiMe_3$), 2.46 (d, J_{PC} = 59.1 Hz, CHP), 45.56 (NMe_2), 58.08 (CH_2N) 115.00, 125.41, 126.77 (Ph), 162.73 (d, J_{PC} = 56.7 Hz, Ph). $^{31}P\{^1H\}$ NMR (d_8-THF, 296 K): δ −67.8.

$[[\{(Me_3Si)_2CH\}(Ph)P]K(pmdeta)]_2$ [17(pmdeta)]. To a solution of **14** (0.94 g, 3.51 mmol) in diethyl ether (20 mL) was added *n*-BuLi (1.40 mL, 3.51 mmol), and this mixture was stirred at room temperature for 1 h. The resulting solution was added to a solution of KO-*t*-Bu (0.39 g, 3.51 mmol) in diethyl ether (20 mL), and this mixture was stirred at room temperature for 1 h. Solvent was

(21) Benet, S.; Cardin, C. J.; Cardin, D. J.; Constantine, C. P.; Heath, P.; Rashid, H.; Teixeira, S.; Thorpe, J. H.; Todd, A. K. *Organometallics* **1999**, *18*, 389.

(22) Wiberg, N.; Wagner, G.; Müller, G.; Riede, J. *J. Organomet. Chem.* **1984**, *271*, 381.

Table 1. Crystallographic Data for **15**(THF), **16**(tmeda), **17**(pmdeta), **18**·Et_2O, **19a**, and **20**

	15(THF)	**16**(tmeda)	**17**(pmdeta)	**18**·Et_2O	**19a**	**20**
formula	$C_{25}H_{48}LiO_3PSi_2$	$C_{38}H_{80}N_4Na_2P_2Si_4$	$C_{44}H_{94}K_2N_6P_2Si_4$	$C_{56}H_{106}Ge_2OP_4Si_8$	$C_{55}H_{104}LiO_4P_3Si_6Sn$	$C_{43}H_{80}GeLiOP_3Si_6$
M_w	490.7	813.3	959.8	1289.2	1216.5	954.1
cryst. size/mm	0.40 × 0.40 × 0.24	0.45 × 0.40 × 0.40	0.25 × 0.20 × 0.20	0.50 × 0.50 × 0.40	0.42 × 0.30 × 0.30	0.40 × 0.40 × 0.20
cryst. syst.	triclinic	triclinic	monoclinic	orthorhombic	cubic	orthorhombic
T/K	150	160	160	150	150	150
space group	$P\bar{1}$	$P\bar{1}$	$P2_1/c$	$P2_12_12_1$	$F\bar{4}3c$	$Pna2_1$
a /Å	9.1099(9)	11.8928(12)	13.538(3)	21.4695(13)	39.504(10)	14.464(5)
b /Å	10.7582(11)	13.3060(13)	13.331(3)	22.5652(13)		21.109(3)
c /Å	17.2892(18)	17.8681(18)	17.801(3)	29.9365(18)		18.2313(14)
α /deg	77.1493(16)	93.371(2)				
β /deg	80.0929(16)	100.996(2)	111.225(14)			
γ /deg	65.3595(15)	111.007(2)				
V /Å^3	1495.6(3)	2566.1(4)	2994.9(11)	14503.1(15)	61649(27)	5566(2)
Z	2	2	2	8	32	4
μ/mm^{-1}	0.194	0.223	0.323	1.082	0.521	0.794
trans. coeff. range	0.927−0.955	0.906−0.916	0.924−0.938	0.614−0.671	0.811−0.860	0.742−0.857
reflns. measd.	13338	22965	13750	130441	36004	49063
unique reflns.	6926	11925	5206	35168	4471	9694
R_{int}	0.020	0.022	0.057	0.065	0.058	0.053
reflns. with $F^2 > 2\sigma$	5321	9215	3448	26086	2961	8332
parameters	324	471	324	1332	235	526
R (on F, $F^2 > 2\sigma$)[a]	0.042	0.048	0.058	0.051	0.055	0.054
R_w (on F^2, all data)[a]	0.112	0.118	0.129	0.121	0.146	0.146
goodness of fit[a]	1.040	1.077	1.075	1.140	1.109	1.070
max, min electron density/e Å^{-3}	0.42, −0.31	0.39, −0.41	0.33, −0.27	1.42, −0.59	0.49, −0.37	1.16, −0.53

[a] Conventional $R = \sum||F_o| - |F_c||/\sum|F_o|$; $R_w = [\sum w(F_o^2 - F_c^2)^2/\sum w(F_o^2)^2]^{1/2}$; $S = [\sum[w(F_o^2 - F_c^2)^2]/(\text{no. data} - \text{no. params})]^{1/2}$ for all data.

removed in vacuo giving a sticky brown solid which was washed with light petroleum (3 × 20 mL) and dried in vacuo, yielding a yellow-orange pyrophoric solid (**17**). Crystals of the adduct **17**(pmdeta) suitable for an X-ray crystallographic study were obtained from hot methylcyclohexane containing 1 equiv of pmdeta. Yield: 0.97 g, 59.5%. Anal. Calcd. for $C_{22}H_{47}KN_3PSi_2$: C, 55.01; H, 9.79; N, 8.75%. Found: C, 54.79; H, 9.60; N, 8.60%. ^{1}H NMR (d_8-THF, 297 K): δ 0.07 (s, 18H, $SiMe_3$), 0.13 (s, 1H, CHP), 2.15 (s, 12H, NMe_2), 2.19 (s, 3H, NMe), 2.31 (m, 4H, CH_2N), 2.42 (m, 4H, CH_2N), 5.96−6.83 (m, 5H, Ph). ^{13}C{^{1}H} NMR (d_8-THF, 297 K): δ 0.84 ($SiMe_3$), 3.83 (d, J_{PC} = 66.2 Hz, CHP), 42.33 (NMe), 45.30 (NMe_2) 56.42 (CH_2N), 57.89 (CH_2N) 111.61, 124.14, 126.47 (Ph), 166.72 (d, J_{PC} = 68.1 Hz, Ph). ^{31}P{^{1}H} NMR (d_8-THF): δ −51.3.

[[{(Me$_3$Si)$_2$CH}(Ph)P]$_2$Ge]$_2$·Et$_2$O (18·Et$_2$O). To a stirred solution of $GeCl_2$(1,4-dioxane) (0.45 g, 1.94 mmol) in THF (20 mL) was added a solution of **17** (1.19 g, 3.89 mmol) in THF (20 mL), and this mixture was stirred at room temperature for 16 h. Solvent was removed in vacuo, and the sticky brown solid was extracted into light petroleum (20 mL) and filtered. Solvent was removed in vacuo from the filtrate, and the sticky solid was crystallized from cold (−30 °C) hexamethyldisiloxane containing a few drops of diethyl ether as orange blocks of the solvate **18**·Et_2O. Yield: 0.76 g, 60.8%. Anal. Calcd. for $C_{52}H_{96}Ge_2P_4Si_8$ (empirical formula without solvent of crystallization): C, 51.40; H, 7.96%. Found: C, 51.27; H, 8.14%. ^{1}H NMR (d_8-THF, 323 K): δ −0.03 (s, 18H, $SiMe_3$), 0.07 (s, 18H, $SiMe_3$), 0.13 (s, 18H, $SiMe_3$), 0.24 (br s, 18H, $SiMe_3$), 0.44 (m, 2H, CHP), 0.53 (m, 2H, CHP), 1.11 (t, ca. 6H, Et_2O), 3.39 (q, ca. 4H, Et_2O), 6.73−8.01 (m, 20H, Ph). ^{31}P{^{1}H} NMR (d_8-THF, 323 K): δ −26.4 (br s, minor), −36.7 (t, $^2J_{PP}$ = 36.0 Hz, minor), −37.3 (t, $^2J_{PP}$ = 17.4 Hz, major), −43.2 (br t, $^2J_{PP}$ = ca. 36 Hz, minor), −50.5 (br t, $^2J_{PP}$ = ca. 33 Hz, minor), −58.1 (t, $^2J_{PP}$ = 17.4 Hz, major).

[[{(Me$_3$Si)$_2$CH}(Ph)P]$_3$SnLi(THF)] (19). To a stirred solution of $SnCl_2$ (0.14 g, 0.74 mmol) in cold (−78 °C) THF (20 mL) was added a solution of **15**(THF) (1.09 g, 2.22 mmol) in THF (20 mL), excluding light as much as possible. The reaction mixture was allowed to attain room temperature and was stirred for 16 h. Solvent was removed in vacuo, and the sticky brown solid was extracted into methylcyclohexane (20 mL) and filtered. The filtrate was cooled to −30 °C to give orange microcrystals of **19**. Yield: 0.51 g, 69.0%. Anal. Calcd. for $C_{43}H_{80}LiOP_3Si_6Sn$: C, 51.64; H, 8.06%. Found: C, 51.47; H, 7.91%. ^{1}H NMR (d_8-toluene, 297 K): δ −1.16 (s, 3H, CHP), 0.13 (s, 54H, $SiMe_3$), 1.59 (br s, 4H, THF), 4.00 (br s, 4H, THF), 6.99−7.97 (m, 15H, Ph). ^{13}C{^{1}H} NMR (d_8-toluene, 297 K): δ 3.03 ($SiMe_3$), 4.04 ($SiMe_3$), 8.24 (d, J_{PC} = 24.9 Hz, CHP), 25.26 (THF), 68.91 (THF), 139.14, 140.28 (Ph, remaining signals obscured by solvent). ^{7}Li{^{1}H} NMR (d_8-toluene, 297 K): δ 3.4 (q, J_{PLi} = 50.8 Hz). ^{31}P{^{1}H} NMR (d_8-toluene, 297 K): δ −47.3 (q, J_{PLi} = 50.8 Hz, J_{PSn} = 747 and 780 Hz). ^{119}Sn{^{1}H} NMR (d_8-toluene, 297 K): δ −105 (q, J_{SnP} = 780 Hz).

[[{(Me$_3$Si)$_2$CH}(Ph)P]$_3$Sn]$^-$[Li(THF)$_4$]$^+$ (19a). Dissolution of **19** in *n*-hexane containing a few drops of THF and cooling to 5 °C for several hours yields crystals of the contact ion pair $[[\{(Me_3Si)_2CH\}(Ph)P]_3Sn]^-[Li(THF)_4]^+$ (**19a**). This compound rapidly reverts to **19** on exposure to vacuum, but NMR data corresponding to **19a** may be obtained in d_8-THF. ^{1}H NMR (d_8-THF, 297 K): δ 0.06 (s, 54H, $SiMe_3$), 1.04 (s, 3H, CHP), 1.81 (br s, 16H, THF), 3.64 (br s, 16H, THF), 6.73−7.73 (m, 15H, Ph). ^{13}C{^{1}H} NMR (d_8-THF, 297 K): δ 2.84 ($SiMe_3$), 6.20 (d, J_{PC} = 30.7 Hz, CHP), 24.43 (THF), 66.59 (THF), 122.63, 125.67, 134.86 (Ph), 149.34 (d, J_{PC} = 39.4 Hz, Ph). ^{7}Li{^{1}H} NMR (d_8-THF, 297 K): δ 2.3 (s). ^{31}P{^{1}H} NMR (d_8-THF, 297 K): δ −46.6 (s, J_{PSn} = 995 and 1038 Hz). ^{119}Sn{^{1}H} NMR (d_8-THF, 297 K): δ 62 (q, J_{SnP} = 1038 Hz).

[[{(Me$_3$Si)$_2$CH}(Ph)P]$_3$GeLi(THF)] (20). To a stirred solution of $GeCl_2$(1,4-dioxane) (0.28 g, 1.21 mmol) in THF (20 mL) was added a solution of **15**(THF) (1.78 g, 3.63 mmol) in THF (20 mL), and this mixture was stirred at room temperature for 16 h. Solvent was removed in vacuo, and the sticky brown solid was extracted into diethyl ether (20 mL) and filtered. Solvent was removed in vacuo from the filtrate, and the sticky solid was crystallized from cold (−30 °C) *n*-hexane containing a few drops of THF as orange blocks of **20**. Yield: 0.61 g, 52.8%. Anal. Calcd. for $C_{43}H_{80}GeLiOP_3Si_6$: C, 54.13; H, 8.45%. Found: C, 54.08; H, 8.40%. ^{1}H NMR (d_8-toluene, 295 K): δ −1.32 (s, 3H, CHP), 0.04 (s, 27H, $SiMe_3$), 0.17 (s, 27H, $SiMe_3$), 1.58 (br m, 4H, THF), 3.93 (br m, 4H, THF), 7.01−8.10 (m, 15H, Ph). ^{13}C{^{1}H} NMR (d_8-toluene, 296 K): δ 2.97 ($SiMe_3$), 4.33 ($SiMe_3$), 8.48

(d, J_{PC} = 23.9 Hz, CHP), 25.29 (THF), 68.78 (THF), 127.65, 128.36, 138.92, 140.13 (Ph). ^{7}Li{^{1}H} NMR (d_8-toluene, 296 K): δ 3.2 (q, J_{LiP} = 50.4 Hz). ^{31}P{^{1}H} NMR (d_8-toluene, 296 K): δ −32.1 (q, J_{PLi} = 50.4 Hz).

[[{(Me$_3$Si)$_2$CH}(Ph)P]$_3$Ge]$^-$[Li(THF)$_4$]$^+$ (20a). Although the separated ion pair complex [[{(Me$_3$Si)$_2$CH}(Ph)P]$_3$Ge]$^-$[Li(THF)$_4$]$^+$ (**20a**) could not be isolated in the solid state because of rapid desolvation to give the contact ion pair **20**, NMR data recorded in d_8-THF are consistent with the presence of the former: ^{1}H NMR (d_8-THF, 296 K): δ −0.12 (s, 54H, SiMe$_3$), 0.68 (m, 3H, CHP), 1.78 (br m, 16H, THF), 3.62 (br m, 16H, THF), 6.86−8.04 (m, 15H, Ph). ^{13}C{^{1}H} NMR (d_8-THF, 297 K): δ 2.75 (SiMe$_3$), 6.29 (d, J_{PC} = 38.4 Hz, CHP), 24.41 (THF), 66.49 (THF), 124.07, 125.78, 137.73, 147.69 (Ph). ^{7}Li{^{1}H} NMR (d_8-THF, 297 K): δ 2.5 (s). ^{31}P{^{1}H} NMR (d_8-THF, 297 K): δ −42.3 (s).

Crystal Structure Determinations of 15(THF), 16(tmeda), 17(pmdeta), 18·Et$_2$O, 19a and 20. Measurements were made on either a Bruker AXS SMART or a Nonius KappaCCD diffractometer using graphite-monochromated MoKα radiation (λ = 0.71073 Å). Cell parameters were refined from the observed positions of all strong reflections. Intensities were corrected semiempirically for absorption, based on symmetry-equivalent and repeated reflections. The structures were solved by direct methods and refined on F^2 values for all unique data. Table 1 gives further details. All non-hydrogen atoms were refined anisotropically, and H atoms were constrained with a riding model; U(H) was set at 1.2 (1.5 for methyl groups) times U_{eq} for the parent atom. Minor disorder was resolved for the two THF ligands in **15**(THF) and for the pmdeta ligand in **17**(pmdeta). In **19a** one THF ligand is disordered by a crystallographic C_3 axis, so the structural model contains one component with 1/3 occupancy. In all three of these structures the disorder does not include the coordinating N or O atoms and so does not impact on the metal coordination geometry. In **20**, there is only one crystallographically independent phosphanide ligand, and this is disordered equally over two orientations. The C and H atoms could not be resolved, as the two components overlap closely, but two alternative positions were successfully refined for the P atom with unequal occupancy; unresolved C/H atom disorder is apparent in large anisotropic displacement parameters. Refinement of disorder components was aided by geometrical similarity restraints for **19a**, and restraints on displacement parameters for **19a** and **20**, but these were unnecessary for the other structures. Programs were Bruker AXS SMART and SAINT or Nonius COLLECT and EvalCCD, and SHELXTL for structure solution, refinement, and molecular graphics.[23]

Acknowledgment. The authors are grateful to the EPSRC for support.

Supporting Information Available: For **15**(THF), **16**(tmeda), **17**(pmdeta), **18**·Et$_2$O, **19a**, and **20** details of structure determination, atomic coordinates, bond lengths and angles, and displacement parameters in CIF format. This material is available free of charge via the Internet at http://pubs.acs.org. Observed and calculated structure factor details are available from the authors upon request.

(23) (a) *COLLECT*; Nonius B. V.: Delft, The Netherlands, 1998. (b) *SMART and SAINT*; Bruker AXS Inc.: Madison, WI, 2004 and 1997; (c) Sheldrick, G. M. *Acta Crystallogr., Sect. A* **2008**, *64*, 112.